Atmos. Chem. Phys. Discuss., 12, 15009–15048, 2012
www.atmos-chem-phys-discuss.net/12/15009/2012/
doi:10.5194/acpd-12-15009-2012

Atmospheric Chemistry and Physics Discussions

The Australian bush fires of February 2009: MIPAS observations and GEM-AQ model results

N. Glatthor[1], M. Höpfner[1], K. Semeniuk[2], A. Lupu[2], P. I. Palmer[3], J. C. McConnell[2], J. W. Kaminski[2], T. von Clarmann[1], G. P. Stiller[1], B. Funke[4], S. Kellmann[1], A. Linden[1], and A. Wiegele[1]

[1]Karlsruher Institut für Technologie, Institut für Meteorologie und Klimaforschung, Karlsruhe, Germany
[2]Centre for Research in Earth and Space Science, York University, Toronto, Canada
[3]School of GeoSciences, University of Edinburgh, Edinburgh, UK
[4]Instituto de Astrofísica de Andalucía (CSIC), Granada, Spain

Received: 5 April 2012 – Accepted: 22 May 2012 – Published: 12 June 2012

Correspondence to: N. Glatthor (norbert.glatthor@kit.edu)

Published by Copernicus Publications on behalf of the European Geosciences Union.

Abstract

On 7 February 2009, and the following days Southeast Australia was devastated by large bush fires, which burned an area of about 3000 km^2. This event was extraordinary, because a large number of combustion products was transported into the uppermost troposphere and lower stratosphere within a few days. Various biomass burning products released by the fire were observed by the Michelson Interferometer for Passive Atmospheric Sounding (MIPAS) on the ENVISAT satellite. We track the plume using MIPAS C_2H_2, HCN and HCOOH single-scan measurements on a day-to-day basis. The measurements are compared with a high-resolution model run of the Global Environmental Multiscale-Air Quality (GEM-AQ) model. Generally there is very good agreement between the spatial distribution of measured and modelled pollutants during the first two weeks after the outbreak of the fire even over intercontinental distances. Both MIPAS and GEM-AQ show a fast south-eastward transport of the pollutants to New Zealand within one day. During the following 3–4 days the plume was located north and eastward of New Zealand and centered at altitudes of 15 to 18 km. Thereafter its eastern part was transported eastward at altitudes of 15–16 km, followed by westward transport of its western part at somewhat higher altitudes. On 17 February the eastern part had reached Southern South America and on 20 February the South African west coast. On the latter day a second relic of the plume was observed moving eastward above the Southern Pacific, whereas the westward transported pollutants were located above Australia at altitudes of 18–20 km. First evidence for entry of the pollutants into the stratosphere was found in MIPAS data of 11 February, followed by larger amounts on 17 February and the days thereafter. Between 20 February and the first week of March the stratospheric pollutants above Australia were transported further westward over the Indian Ocean towards Southern Africa.

1 Introduction

Biomass burning is a major source of tropospheric pollution (Singh et al., 1996, 2000; Li et al., 2003) in addition to other anthropogenic sources. While the main species produced are CO_2, water vapour and smoke, a large suite of short-lived and longer-lived organic and a few inorganic species are also generated. Important biomass burning products are carbon monoxide (CO), ethane (C_2H_6), acetylene (C_2H_2), methanol (CH_3OH), hydrogen cyanide (HCN), acetonitrile (CH_3CN), peroxyacetyl nitrate (PAN, $CH_3C(O)OONO_2$) and formic acid (HCOOH). HCN and CH_3CN are nearly exclusively produced by biomass burning (Li et al., 2003; Singh et al., 2003; Yokelson et al., 2007; Lupu et al., 2009). Fire-induced convection or favourable meteorological conditions can cause significant amounts of these pollutants to be transported into the free troposphere (Donnell et al., 2001; Kahn et al., 2007). Thus, since the tropospheric lifetime of most of these trace gases is several weeks, they can form upper tropospheric plumes persisting over time periods of the same order. A prominent example is the southern hemispheric biomass burning plume caused by continuous combustion throughout the dry season in South America, Central and Southern Africa and Australia, which regularly peaks between September and November. The spatial extension and composition of this plume has been investigated using various ground based, airborne and spaceborne observations (Singh et al., 1996, 2000; Rinsland et al., 2001, 2005; von Clarmann et al., 2007; Glatthor et al., 2009). Another region of long-lasting upper tropospheric pollution is the Asian monsoon anticyclone, which typically appears above Southern Asia in June, July and August (Park et al., 2008). Due to the relatively low signal-to-noise ratio and cloud contamination, temporal and spatial averaging has been performed for the larger part of spaceborne observations published so far for biomass burning.

At the beginning of February 2009, the state of Victoria in Southeastern Australia was devastated by the most disastrous bush fires in terms of the number of fatalities (173 people died), which had ever taken place in Australia (Tolhurst, 2009). The total burned

area amounted at about 3000 km^2, most of it was burned on 7 February 2009, the so-called "Black Saturday". The largest of these fires was the Kilmore East fire 85 km north of Melbourne. The fire, caused by a failure of electrical powerlines, started around midday local time on 7 February and was declared contained on 16 February (Teague et al., 2010). An area of about 1250 km^2 was burned, the major part of it (1150 km^2) on 7 February (Tolhurst, 2009). The fire-driven convection was sufficient to loft the pollutants high into the troposphere, and further enhanced by a low pressure trough, which passed over the area ahead of a cold front and lead to an unstable atmosphere. At around 19:30 LT the fire-induced pyrocumulus cloud was estimated to be 8.5 km high (Tolhurst, 2009), but it likely penetrated to higher altitudes in the following night. Within three days after the fire the smoke plume had drifted to the north of New Zealand and was further lifted to altitudes of 15–20 km, which made this fire an extraordinary event. The mechanism for this subsequent lifting is still under investigation. de Laat et al. (2012) propose heating of the smoke or aerosol particles by shortwave solar radiation.

Detection of combustion products of this event in the upper troposphere and lower stratosphere by the Microwave Limb Sounder (MLS) on Aura has been reported by Pumphrey et al. (2011). They pointed out the unusual injection height of the pollutants reaching up into the stratosphere. MLS observed a CO plume, which was located north and eastward of New Zealand during the first week after the outbreak of the fire. In the second week the CO plume extended up to 46 hPa (~ 21 km) and was distorted in a south-eastern direction. In the following two weeks the stratospheric portion of the plume was observed drifting westward over Australia and the Indian Ocean. In a statistical investigation Pumphrey et al. (2011) documented the uniqueness of this event in the MLS data set with respect to injection height. MLS observations are supported by measurements of the Optical Spectrograph and Infrared Imager System (OSIRIS) instrument on the Odin satellite (Siddaway and Petelina, 2011). This instrument observed smoke particles from the Australian fire entering the lower stratosphere around 11 February 2009. Driven by the westward phase of the quasi-biennial

oscillation (QBO) these particles travelled westward in the southern tropics and circled the globe in about 6 weeks (Siddaway and Petelina, 2011). In another paper Clarisse et al. (2011) report on signatures of various biomass burning products detected in nadir spectra of the Infrared Atmospheric Sounding Interferometer (IASI) obtained in the plume of the Australian bush fires.

The Australian bush fire plume was a rather isolated event not much disturbed by other fires, since the southern hemispheric biomass burning plume caused by widespread combustion in South America and Southern Africa has widely disappeared by this time of the year (cf. Glatthor et al., 2009). Further the plume reached extraordinarily high altitudes, where clouds are less frequent allowing a better sampling of the atmosphere by infrared satellite limb measurements. In this paper we study the event using measurements of C_2H_2, HCN and HCOOH by the Michelson Interferometer for Passive Atmospheric Sounding (MIPAS) on ENVISAT in comparison with high-resolution simulations of the GEM-AQ model, which was run for the time period 7 February to 31 March 2009. HCN is a nearly unambiguous tracer of biomass burning (Li et al., 2003; Singh et al., 2003; Yokelson et al., 2007). C_2H_2 is another, although not unambiguous biomass burning tracer (Singh et al., 1996), and HCOOH has additional, e.g. biogenic tropospheric sources (Keene and Galloway, 1988; Grutter et al., 2010; Stavrakou et al., 2012). The upper tropospheric lifetime of HCN is $\sim$ 5.3 months (Li et al., 2003; Lupu et al., 2009). Respective data for the lifetime of C_2H_2 vary between two weeks (Xiao et al., 2007) and 50 days (Rudolph et al., 1984), and for HCOOH between several days and a few weeks (Grutter et al., 2010). Further, using GEM-AQ OH profiles we have estimated a C_2H_2 lifetime of about 3 weeks in the lower stratosphere. In this paper we will discuss single-scan MIPAS measurements to study the day-to-day evolution and expansion of the plume and to evaluate the model results. In Sects. 2 and 3 we will describe the technical aspects of the MIPAS measurements, the retrieval and the GEM-AQ model, respectively. In Sect. 4 we will use measured and model data to analyze the transport and dilution of the pollutants. In Sect. 5 we will summarize

the detected transport pattern, evaluate the comparison between MIPAS and GEM-AQ results and discuss the implications for future measurements.

2 MIPAS Measurements

On 1 March 2002 the European ENVIronmental SATellite (ENVISAT) was launched into a sun-synchronous polar orbit at about 800 km altitude. The satellite performs 14.3 orbits per day and passes the equator at $\sim$ 10 : 00 LT and $\sim$ 22 : 00 LT. Among various other experiments, ENVISAT hosts the Michelson Interferometer for Passive Atmospheric Sounding (MIPAS). MIPAS is a limb-viewing Fourier transform infrared (FTIR) emission spectrometer covering the mid-infrared spectral region between 685 and 2410 cm^{-1} (4.1–14.6 µm), which enables simultaneous observation of numerous trace gases (European Space Agency (ESA), 2000, Fischer et al., 2008).

Since March 2004 MIPAS has been operated in the so-called optimal resolution (OR) measurement mode with a spectral resolution of 0.121 cm^{-1} (full-width at half maximum after Norton Beer "strong" apodization) and a latitudinal sampling distance of $\sim$3.6° (400 km). The across-track coverage of MIPAS is 30 km. We present data of the OR "nominal" measurement mode, consisting of rearward limb-scans covering the altitude region between 7 and 72 km within 27 altitude steps. The step-width is 1.5 km up to 22 km, 2 km up to 32 km, 3 km up to 44 km and 4–4.5 km for the upper end of the scan. MIPAS is able to measure during day and night, and produces up to 1400 scans per day in OR nominal mode. The level-1B radiance spectra used for retrieval are data version 4.67 (reprocessed data) provided by the European Space Agency (ESA) (Nett et al., 2002).

2.1 Retrieval method and error estimation

We present C_2H_2, HCN and HCOOH distributions and additionally C_2H_6, PAN and CO profiles measured by MIPAS-ENVISAT. The respective data versions are

V4O_C2H2_200, V4O_HCN_201, V4O_HCOOH_200, V4O_C2H6_200, V4O_PAN_200 and V4O_CO_200 of the MIPAS OR mode. Processing of MIPAS data at IMK has been described in various papers (von Clarmann et al., 2003, Höpfner et al., 2004). Further, retrieval of C_2H_2, HCN, HCOOH and CO has been discussed by Wiegele et al. (2012), Glatthor et al. (2009), Grutter et al. (2010) and Funke et al. (2009). Therefore we will give only a short description of the retrieval setups here.

The datasets were produced with the retrieval processor of the Institut für Meteorologie und Klimaforschung and the Instituto de Astrofísica de Andalucía (IMK/IAA). Radiative transfer calculations were performed with the Karlsruhe Optimized and Precise Radiative Algorithm (KOPRA) (Stiller, 2000) and the retrievals with the Retrieval Control Program (RCP). The retrievals consist of inversion of MIPAS level-1B spectra to vertical profiles of atmospheric state parameters by constrained non-linear least squares fitting in a global-fit approach (von Clarmann et al., 2003). Tikhonov's first derivative operator is used as constraint (Steck, 2002, and references therein). A constraint is necessary to attenuate instabilities, since the retrieval grid has a finer altitude spacing than the height distance between the tangent altitudes. To avoid any influence of the a-priori information on the shape of the retrieved profiles, height-constant a-priori profiles were chosen. For retrieval of C_2H_2 and HCN an O_3 profile was joint-fitted, and for retrieval of HCOOH we joint-fitted O_3, CFC-11 and CFC-22. Further retrieval parameters were microwindow-dependent continuum radiation profiles and microwindow-dependent, but height-independent zero-level calibration corrections. To account for other contaminating gases, their profiles as retrieved earlier in the processing sequence were used. If no prefitted profiles were available, we used the data of the MIPAS climatology (Remedios et al., 2007).

Figure 1 shows MIPAS single-scan profiles of C_2H_2, HCN, C_2H_6, PAN, HCOOH and CO obtained at three different geolocations. The first set of profiles was measured on 7 February over the Southern Pacific in an unpolluted atmosphere (top left), and the two other sets on 17 February 2009, inside the Australian plume (middle and bottom left). All profiles measured in the unpolluted atmosphere (top left) are close to zero

except for CO, HCN and partly for C_2H_6. CO amounts to 40 ppbv at 13 km, and HCN has a nearly height-constant profile of 200–230 pptv, which is due to its atmospheric lifetime of ∼ 5.3 months in the troposphere (Li et al., 2003) and ∼ 2.5 yr in the stratosphere (Cicerone and Zellner, 1983). The background C_2H_6 profile oscillates distinctly around zero. Inside the plume (middle and bottom left) each of the six pollutants has a pronounced maximum in the height region between 16 and 18 km. There is a remarkable agreement between the profile shapes of the different biomass burning products. The maximum values range from 100 pptv (C_2H_2, C_2H_6) to 500 pptv for HCN and to 100 ppbv for CO, and are generally well above background values. Further, the maxima are all above the tropopause (dashed curves) derived from MIPAS temperature profiles. Whereas the amounts of CO, C_2H_2, C_2H_6 and HCOOH decrease to zero above 23 km, the mid-stratospheric HCN amounts are 150–200 pptv as in the unpolluted case.

Except for C_2H_6, the maxima of all pollutants distinctively exceed the estimated standard deviation resulting from the retrieval (Fig. 1, right row). Compared to the other species the estimated standard deviation (ESD) of C_2H_6 is unusually high. More detailed error analyses of the different species including systematic errors are presented in Wiegele et al. (2012). The vertical resolution of C_2H_2 and PAN is ∼ 3.5 km at 15 km and ∼ 6.5 km at 21 km altitude. The respective values are 4 km and 6.5 km for HCOOH, 4.5 km and 6 km for HCN, 5 km and 8 km for C_2H_6 and 6 km and 6.5 km for CO.

In Table 1 we list mean values, standard deviations (σ) and upper thresholds for strong outliers for "background" distributions of southern hemispheric C_2H_2, HCN and HCOOH averaged over the time period 1 January to 7 February 2009. C_2H_2, HCN and HCOOH amounts exceeding the given thresholds can be attributed to fresh pollution events with high confidence.

2.2 Uniqueness of the Australian plume

To point out the uniqueness of the Australian bush fire with respect to plume height, Fig. 2 shows two time series of MIPAS C_2H_2 data from the latitude band between the equator and 60° S, measured at 18 and 21 km altitude. Both datasets exhibit

background values of up to 30 pptv until the outbreak of the fire (day 37, 7 February) and from about day 75 (17 March) until the end of the displayed time period (31 October). After the outbreak of the fire there is an abrupt increase of maximum C_2H_2 amounts of up to 280 pptv at 18 km and a somewhat slower increase of up to 130 pptv at 21 km altitude, lasting for some weeks. The C_2H_2 data peak at days 43–44 (13–14 February) at 18 km altitude and around day 59 (1 March) at 21 km altitude. At both altitudes enhanced C_2H_2 values persist until mid-March. The time series also includes the peak of the main southern hemispheric biomass burning season in October. It is evident that pollutants released during September and October did not reach such high altitudes.

3 GEM-AQ model setup

In order to simulate the release of pollutants by the "Black Saturday" fires, we used the Global Environmental Multiscale Air Quality (GEM-AQ) model (Kaminski et al., 2008), a tropospheric chemistry, general circulation model based on the global variable resolution multiscale GEM model developed by the Meteorological Service of Canada for operational weather prediction (Côté et al., 1998a, b). The version of GEM-AQ employed in this study uses GEM version 3.3.2 with physics package version 5.0.4 and was run in global variable (GV) mode, i.e. with a uniform interior grid. All species are advected using the semi-Lagrangian scheme native to GEM. The vertical transport includes parameterized subgrid scale turbulence and deep convection. Dry deposition is included as a flux boundary condition in the vertical diffusion equation. Both in-cloud and below-cloud scavenging are considered. The original chemistry mechanism described in Kaminski et al. (2008) was expanded to include HCN loss processes (Lupu et al., 2009) and production of HCOOH via reactions initiated by $HCHO + HO_2$. No aerosol physics and chemistry were implemented in this version of the model. The GEM-AQ has been validated by comparison with spaceborne, airborne and ballonborne observations.

The model run was focused on the largest of the Victorian fires, the Kilmore East fire on 7 February 85 km north of Melbourne. The model fire distribution was taken from the Royal Commission report (Teague et al., 2010). Calculations by the PHOENIX RapidFire fire spread model (Tolhurst et al., 2008) suggest that the total heat output of the fire on 7 February was 53 PJ (Tolhurst, 2009). Assuming a standard heat of combustion of 18.7 $MJ\,kg^{-1}$ for forest fuel (Trentmann et al., 2006) and a carbon content of 0.48 $kg\,C\,kg^{-1}$ dry fuel (van der Werf et al., 2010), we estimated a total emission of 1.4 Tg C. Our estimated total and specific emissions are in agreement with recently published values from the GFED3 daily database (Mu et al., 2011). Based on this amount, and by using biome-dependent emission factors (M. O. Andreae, personal communication 2009; Andreae and Merlet, 2001), we quantified emissions for 23 pyrogenic species, all of which were included in the simulation. In particular we estimated HCN at 2.3 Gg, C_2H_2 at 0.7 Gg, and HCOOH at 1.0 Gg. Background emissions (yearly-averaged for anthropogenic and monthly-averaged for biogenic emissions and biomass burning) used in the GEM-AQ simulation are from Kaminski et al. (2008).

The model was run from 7 February to 31 March 2009. The run consisted of a simulation at 50 km horizontal and $\sim$ 300 m vertical resolution (middle and upper troposphere) to study the global impacts. The evolution of the pyroconvection plume could not be properly simulated due to lack of sufficient resolution to resolve convective turbulence, absence of 3-D radiative transfer and missing aerosol radiative effects (including those suggested by de Laat et al., 2012). Instead the initial plume was prescribed as a grid box column. The pyrogenic emissions were distributed between 14 and 18 km in order to produce the lofting of the plume into the stratosphere. The column injection was switched on at 15:00 UT on 7 February and maintained for 9 h.

These simplifications were necessitated by lack of observations of plume height during the night of 7 February. We obtained a reasonable correspondence between the observed and modeled plume transport in the subsequent weeks. A simulation where the emissions were distributed below 8.5 km failed to transport tracers above 16 km. It is unlikely that the Kilmore East pyroconvection only rose to 8.5 km. Except for the

altitude distribution, the initial plume release details appear to be of secondary importance.

To enable comparison with observations, the model was re-initialized every 24 h with analysis data. A six hour adjustment period was used to ingest analysis winds and temperatures without chemistry and transport of species. Chemistry and species transport were switched on for a 24 h period following the adjustment period and using the output from the end of the previous day as input. For the investigations presented in this paper model data with output saved every 6 h were available. In the Supplement we present an animation of the expansion of the model HCN 450 pptv isosurface in original resolution during the first two weeks after the outbreak of the fire.

Smoothing of model data

To compare with MIPAS data the model fields were convolved with horizontal and vertical averaging kernels representative for the biomass burning products measured by MIPAS. For this purpose, the irregularly gridded model data were first interpolated onto a regular grid with latitudinal and longitudinal spacing of 0.5° and a vertical sampling of 1 km. Then each gridpoint of this field was convolved with a triangular weighting function with a vertical full-width at half maximum (FWHM) of 5 km and a latitudinal FWHM of 300 km. The width of the applied vertical smoothing function is the average height resolution of the different gases for the altitude region 15 to 21 km (cf. Sect. 2.1) and the width of the applied horizontal smoothing function is at the upper end of the values given in von Clarmann et al. (2009).

After degradation to MIPAS resolution fine-scale structures of the original GEM-AQ distributions become blurred to a certain degree. For example, latitudinal cross sections of modelled C_2H_2 of 11 February 2009, exhibit two separated maxima at ~ 175° W, one at 30° S at 17.5 km altitude and another at 25° S at 16 km (not shown). This structure is strongly washed-out after convolution with MIPAS averaging kernels. Nevertheless, MIPAS also observed two maxima at different altitudes (17 and 13 km) at approximately the same time and location (cf. Fig. 11, upper left panel).

4 Comparison of measured and modelled plumes

The GEM-AQ model run lasted from 7 February to 31 March 2009. Except for a few days (e.g. 15 and 16 February) MIPAS data are available for the whole time period. We compare the spatial propagation of the measured and modelled plumes mainly for the first two weeks after the fire event. For this purpose we discuss the C_2H_2, HCN and HCOOH distributions from 8, 9, 11, 14, 17 and 20 February at altitudes of 15, 18 and 21 km, with the last height being approximately equivalent to the highest pressure level of ~ 46 hPa discussed in Pumphrey et al. (2011). The comparison is focused on these three gases, because the MIPAS data for these species exhibit a large contrast between plume and background values. The model distributions shown are always from 12:00 UT, whereas MIPAS data vary between 00:00 and 24:00 UT. In Sect. 4.5 we additionally compare measured and modelled stratospheric C_2H_2 over a longer time period until 11 March.

4.1 C_2H_2 distributions

Figure 3 shows the measured and modelled C_2H_2 distribution at the altitude of 15 km. On 8 February the GEM-AQ plume is situated above Southern New Zealand (Fig. 3, top left), whereas MIPAS observed only background values at this altitude (the threshold for elevated values is 56 pptv, cf. Table 1). MIPAS measured enhanced C_2H_2 of up to 110 pptv at the lower altitude of 12 km to the east and northeast of New Zealand instead (Fig. 6). This discrepancy might be due to the direct injection of the major part of the pollutants into the UTLS by the model, which was necessary to create a plume at altitudes consistent with the observations of the following days, but it can also be a sampling problem of MIPAS (cf. Sect. 2). The C_2H_2 values observed at about 12:00 UT are located at the edge of the GEM-AQ plume from 15 km only, and the two data points covering the western part of the plume were measured at 23:00 UT, when the GEM-AQ pollutants had moved considerably further eastward. On the other hand, at 12 km the model plume is displaced somewhat further to the east, where the

enhanced C_2H_2 data points of MIPAS from this altitude were measured. Lidar data of the Cloud-Aerosol Lidar and Infrared Pathfinder Satellite Observations (CALIPSO) satellite of 8 February also exhibit an aerosol plume over New Zealand reaching up to 12 km only, but they are from 02:00 UT and probably obtained somewhat too far east ($\sim 178^\circ$ W).

On 9 February the GEM-AQ plume is more elongated, stretching from the east to the north of New Zealand. On this day MIPAS measured one strongly enhanced C_2H_2 value of ~ 150 pptv at the northwestern edge of the model plume. During the following days the major part of the pollutants remained to the north an northeast of New Zealand. MIPAS also observed spatially distributed elevated C_2H_2 values on 11 February, slightly displaced into southwesterly direction as compared to the model. By 14 February the center of the model plume has moved far southeast and starts turning northward, whereas its western end is still north of New Zealand. The same structure is visible in enhanced MIPAS C_2H_2 data of comparable magnitude. There is even agreement in the northward turn of the plume at 240° E, although the MIPAS data are somewhat ahead. On 17 February the centers of measured and modelled C_2H_2 plumes have moved to Southern South America. Further, both datasets show a secondary maximum over the Pacific at 210° E. Whereas the remains of the model plume north of New Zealand are largely diluted, there are still enhanced MIPAS data somewhat further north. According to MIPAS and GEM-AQ the maximum above South America has moved further eastward to the South African west coast on 20 February. Further, both datasets exhibit enhanced values in a long north-southward stripe over the Southern Pacific on this day, which is a second eastward travelling plume relic.

For the first three of the days presented the GEM-AQ volume mixing ratios are much higher than those of MIPAS even after smoothing with the MIPAS averaging kernels (cf. Table 2). For example, smoothed model C_2H_2 vmrs on 9 February are up to ~ 830 pptv at 15 km altitude, whereas the highest C_2H_2 amount measured by MIPAS at this height is ~ 150 pptv. Possible reasons for the higher model values are direct injection of the simulated plume into the UTLS, the magnitude of the fire emissions used or too coarse

spatial sampling of MIPAS. Between 14 and 20 February the mixing ratios at 15 km agree much better. On 14 February the model values inside the plume range from 100 to 370 pptv and the measured values from 100 to 215 pptv, and on 17 February maximum modelled and measured values are consistently between 200 and 220 pptv.

Most of the measured and modelled features of the C_2H_2 distributions at 18 km altitude (Fig. 4) are similar as at 15 km. On 8 February the model plume is located over New Zealand, showing fast southeastward transport. The first two enhanced MIPAS C_2H_2 values of up to 140 pptv were observed one day later at the north-western edge of the model plume (the threshold for enhanced values is 20 pptv, cf. Table 1). There is similar good spatial agreement for 11 and 14 February as at 15 km altitude. Again, the model distribution exhibits maximum values above Southern South America on 17 February, whereas MIPAS measured only moderately enhanced amounts in this region. On this day stronger enhanced MIPAS C_2H_2 amounts were observed north- and eastward of New Zealand, which spatially coincide well with two weaker maxima of the model distribution. On 20 February both datasets exhibit the north-southward expanded relic of the plume over the Southern Pacific around 250° E and the maximum at the South African west coast. In addition, MIPAS and GEM-AQ show westward transported enhanced C_2H_2 vmrs at the Australian east coast. Like at 15 km the GEM-AQ plume mixing ratios are much higher than those of MIPAS during the first three days presented, of the same magnitude on 14 February (both datasets ~ 280 pptv) and somewhat smaller on 17 and 20 February (cf. Table 2).

At 21 km the modelled C_2H_2 amounts are smaller than at 15 and 18 km, up to 125 pptv on 8 February and up to ~ 180 pptv on 9 February (Fig. 5). MIPAS observed the first moderately enhanced C_2H_2 value (45 pptv) at the western edge of the model plume on 11 February. At this altitude eastward transport is much less distinct than at 15 and 18 km. Westward transport towards Australia becomes dominant instead. The model plumes of 14, 17 and 20 February north of New Zealand and above the Australian east coast are well covered by enhanced MIPAS C_2H_2 values. Similar to lower altitudes the modelled plume mixing ratios are higher than the measured amounts on

the first four days presented, but there is good agreement on 17 and 20 February (cf. Table 2).

4.2 HCN distributions

The measured and modelled HCN plumes at 18 km altitude (Fig. 7) correspond well with the respective C_2H_2 distributions. Practically all enhanced MIPAS HCN values are at exactly the same geolocations as the elevated measured C_2H_2 data. This is as expected, reflecting the fact that the stratospheric lifetimes of both species are three weeks (C_2H_2) or longer (HCN), but it also illustrates the data quality of MIPAS. Further, measured HCN is also consistent to the modelled HCN plume during most of the days presented. The modelled HCN plume also is located above Southern New Zealand on 8 February, whereas the first significantly enhanced MIPAS HCN value of ∼ 480 pptv was measured on 9 February at the northwestern edge of the model plume (threshold for enhanced values is 365 pptv, cf. Table 1). However, as discussed in Sect. 4.1 this discrepancy between model and measurements can just be caused by the coarse spatial sampling of MIPAS. Measurements and model data of 11 February again show the persistence of the plume northeastward of New Zealand. Then the pollutants from the eastern end of the GEM-AQ plume move eastward towards Southern South America and over the Southern Atlantic, followed by a second pulse moving towards South America on 20 February. The western end of the model plume is transported westward towards Australia during the last two days presented. All these model features are well covered by enhanced MIPAS HCN values.

The modelled HCN amounts in the plume are also much larger than the measured values during the first days after the fire. For example on 9 February modelled HCN at 18 km peaks at ∼ 3 ppbv and MIPAS HCN at ∼ 0.5 ppbv. MIPAS background HCN data are between 200 and 300 pptv, whereas the model background values vary between 100 and 260 pptv. Both the measured and modelled distributions indicate regions of moderately enhanced HCN in the tropics caused by other pollution events.

4.3 HCOOH distributions

Figures 8–10 show measured and modelled HCOOH at 15, 18 and 21 km altitude. In addition to the "Australian" plume the model distribution contains an extended plume above tropical South America and two further plumes above the Central Pacific and Northern Australia. Again, the modelled Australian HCOOH plume appears above New Zealand on 8 February, whereas the first measurements of enhanced HCOOH at 15 and 18 km (260 and 175 pptv, respectively) were on 9 February at the northwestern edge of the model plume and at 21 km on 11 February. Between 14 and 20 February the modelled HCOOH plume splits up and is transported eastward and westward in the same way as observed in C_2H_2 and HCN. Nearly all model features are well covered by elevated MIPAS HCOOH values, and the locations of elevated MIPAS HCOOH are largely congruent with those of enhanced C_2H_2 and HCN. Measured and modelled HCOOH also indicates penetration of the plume well into the stratosphere on 11, 14, 17 and 20 February.

However, in the regions of the model plumes over tropical South America, the equatorial Pacific and Northern Australia the model and the measurements disagree. As a result of the rapid isoprene oxidation by OH and the details of the breakdown reaction scheme which produces HCOOH in GEM-AQ, the model exhibits strongly enhanced HCOOH in these regions even at 18 km altitude, whereas the corresponding MIPAS data are consistently lower than those measured in the Australian plume region. For example, on 14 and 17 February modelled HCOOH amounts at 18 km over tropical South America and westward of Peru are of the same order as inside the Australian plume on 14 and 17 February, whereas MIPAS measured enhanced values in the Australian plume only. Elevated MIPAS HCOOH amounts around tropical South America were rather found at 12 km altitude. Obviously the model convective scheme (Kain-Fritsch) causes too much overshooting into the tropical transition layer (TTL).

4.4 Identification of stratospheric C_2H_2 in MIPAS data

Some days after the Australian bush fire event of 7 February 2009, MIPAS measured enhanced amounts of C_2H_2, HCOOH and of other pollutants at altitudes of up to 21 km, which implies a more or less direct transport of biomass burning products into the stratosphere. Indication for stratospheric C_2H_2 and HCOOH is most pronounced on 14 and 17 February, but also on 11 and 20 February (cf. Figs. 5 and 10). To exclude just apparent penetration into the stratosphere caused by smearing effects due to the restricted vertical resolution of observed MIPAS biomass burning products ($\sim$ 5 km at these altitudes) we checked the measured C_2H_2 data for maxima above the tropopause.

As a result of this process Fig. 11 shows the geometrical height of the maxima of C_2H_2 profiles. Maxima situated 1 km or more above the tropopause are underlined, and for more clarity only elevated values above 50 pptv are plotted. The tropopause height was derived from the MIPAS temperature profile using the WMO definition for the thermal tropopause, which is the "lowest level at which the lapse rate -dT/dz is lower than 2 K/km and stays below this value at least for 2 km above this level". On 11 February (top left) there are two data points east of New Zealand indicating stratospheric C_2H_2 at 17 and 18 km altitude. The largest clusters of subtropical to low mid-latitude locations of stratospheric C_2H_2 were observed north and eastward of New Zealand on 17 and 18 February. This is in good agreement with the observations of Pumphrey et al. (2011, Fig. 2). However, on 20 and 21 February MIPAS additionally observed stratospheric C_2H_2 in the region of the southern end of South America.

Figure 11 also gives a general overview of the spatial and temporal variation of plume altitude. On 11 February the plume east of New Zealand is centered at 17 km, but there is another part north of New Zealand at 13–14 km only. The portion of the plume observed on 17 and 18 February north of New Zealand is at $\sim$18 km altitude, whereas the second maximum northeast of New Zealand is centered at 17 km. Further, the first part of the plume arriving over Southern South America on 17 February obviously

was tropospheric, whereas the second fragment following on 20 February was stratospheric. The altitude of the stratospheric pollutants transported westward towards Australia increases from 18 to 19–20 km, which might be an indication for observation of the solar escalator mechanism proposed by de Laat et al. (2012).

4.5 Westward drift of the stratospheric HCN plume

The further history of the stratospheric pollutants observed on 17 February northward of New Zealand is illustrated by presentation of HCN at 21 km altitude (Fig. 12). On 21 February enhanced measured stratospheric HCN as well as the model plume have moved in north-westerly direction towards the southern tropics and are situated above Central Australia, and on 24 February they have reached the Australian west coast. The observed westward transport in the tropical latitude band is caused by the westerly phase of the quasi-biennial oscillation (QBO) during spring 2009 (Siddaway and Petelina, 2011). On 27 February enhanced HCN amounts were measured above the Central Indian Ocean and on 1 March at the South African east coast indicating further westward drift of the "Australian" pollutants, which is in good spatial agreement with the model plume. On 6 March MIPAS still measured high HCN of about 500 pptv above Southern Africa, which is about two times larger than the remains of the model plume. As already outlined in Sect. 1 these MIPAS observations are also confirmed by MLS data (Pumphrey et al., 2011) and by the OSIRIS instrument on the Odin satellite, which measured lower stratospheric smoke particles travelling westward on the same path as MIPAS trace gases (Siddaway and Petelina, 2011).

5 Conclusions

The strong Australian bush fires of 7 February 2009, caused a direct injection of large amounts of various biomass burning products into the upper troposphere. After a few days these pollutants were transported further upward to extraordinarily high altitudes

of 15–20 km, i.e. at least partly into the lower stratosphere. Various combustion products of this fire event were observed by MIPAS on ENVISAT. We presented MIPAS C_2H_2, HCN and HCOOH single-scan data on a day-to-day basis in comparison with simulations of a high-resolution run of the GEM-AQ model mainly for the period 7 to 20 February 2009. Further we investigated more in detail, at which times and locations the troposphere-to-stratosphere transport of parts of the plume occurred.

The first MIPAS observation of upper tropospheric pollution caused by the Australian bush fires was on 8 February at 10 to 12 km altitude north-eastward of New Zealand. The fast eastward transport of pollutants is confirmed by GEM-AQ model data, which at this day show the plume over Southern New Zealand centered at higher altitudes of 15 to 18 km. The height difference between enhanced MIPAS and GEM-AQ data of this day might be caused by direct injection of the model plume into the UTLS region, but can also be a sampling problem of MIPAS. CALIPSO lidar data of 8 February show aerosols up to 12 km only (de Laat et al., 2012), but they also do not cover the center of the plume. On 9 February, MIPAS measured pollution at 15 and 18 km in a localized region at the north-western edge of the model plume, which now extended from the east to north of New Zealand. Thereafter MIPAS also observed spatially extended C_2H_2, HCN and HCOOH distributions at 15 and 18 km in good consistency with the modelled plume. During the next days the plume persisted north-eastward of New Zealand. Then its eastern part was transported eastward at altitudes of 15–16 km, reaching Southern South America on 17 February and the South African west coast on 20 February. On the latter day another relic of the plume moved eastward above the Southern Pacific, and the western part of the plume had reached Eastern Australia at 18–20 km altitude. The good consistency between the spatial coverage and propagation of the measured and modelled Australian plumes confirms the model simulation with respect to plume mapping as well as the reliability of MIPAS single-scan data of biomass burning gases.

During the first 4–5 days after the outbreak of the fire the model volume mixing ratios of the biomass burning products at 15–18 km are much higher than those of MIPAS, whereas there is better agreement on 17 and 20 February. One reason for the

high model values is probably direct injection of the major part of the simulated plume into this height region. MIPAS data indicate that a certain portion of the pollutants also spreads at altitudes of 10–12 km. Other possible reasons for the differences are the estimate of too high fire emissions, but also too coarse sampling of the plume by MIPAS. Further, strongly enhanced HCOOH model data in the TTL above tropical South America are probably caused by the isoprene oxidation mechanism and a too strong convective scheme for these sources.

Only some days after the fire significant amounts of pollutants were measured at altitudes of up to 21 km, which implies a direct transport into the stratosphere. To exclude just apparent entry into the stratosphere caused by the restricted height resolution of the measurements, the datasets were filtered for profiles with maxima above the tropopause. Stratospheric pollution was first identified near New Zealand at 11 February and to a larger extent over the subtropical and mid-latitude Southern Pacific mainly between 17 and 21 February. MIPAS as well as GEM-AQ data from 21 February to 6 March show the westward drift of stratospheric HCN over Australia and the Indian Ocean to Southern Africa. These observations are confirmed by MLS data and measurements of OSIRIS on the Odin satellite.

This comparison of a single biomass burning episode captured by MIPAS with a model simulation of that episode is illuminating. It suggests that observations with a better spatial coverage, say with a tomographic capacity could better characterise the plume dimensions as well as plume height. In this manner, with more comprehensive tracking one might better estimate the amount of biomass burnt as well as its composition.

Acknowledgements. The authors like to thank the European Space Agency for giving access to MIPAS level-1 data. Meteorological analysis data have been provided by ECMWF. GEM-AQ model runs were performed in the frame of the ESA study "PREMIER Consolidation of Requirements and Synergistic Retrieval Algorithms" (contract number 22848/09/NL/CT). J. C. McConnell, K. Semeniuk, A. Lupu and J. W. Kaminski acknowledge support from the IMPACTS contract (number 4000101294/10/NL/CBi) and also Canadian Space Agency grants.

The service charges for this open access publication
have been covered by a Research Centre of the
Helmholtz Association.

References

Andreae, M. O. and Merlet, P.: Emission of trace gases and aerosols from biomass burning, Global Biogeochem. Cy., 15, 955–966, doi:10.1029/2000GB001382, 2001.

Cicerone, R. J. and Zellner, R.: The atmospheric chemistry of hydrogen cyanide (HCN), J. Geophys. Res., 88, C15, 10689–10696, 1983.

Clarisse, L., R'Honi, Y., Coheur, P.-F., Hurtmans, D., and Clerbaux, C.: Thermal infrared nadir observations of 24 atmospheric gases, Geophys. Res. Lett., 38, L10802, doi:10.1029/2011GL047271, 2011.

Côté, J., Gravel, S., Méthot, A., Patoine, A., Roch, M., and Staniforth, A.: The operational CMC-MRB Global Environmental Multiscale (GEM) model. Part I: Design considerations and formulation, Mon. Weather Rev., 126, 1373–1395, 1998a.

Côté, J., Desmarais, J.-G., Gravel, S., Méthot, A., Patoine, A., Roch, M., and Staniforth, A.: The operational CMC-MRB Global Environmental Multiscale (GEM) model. Part II: Results, Mon. Weather Rev., 126, 1397–1418, 1998b.

de Laat, A. T. J., Stein Zweers, D. C., Boers R., and Tuinder O. N. E.: A solar escalator: observational evidence of the self-lifting of smoke and aerosols by absorption of solar radiation in the February 2009 Australian Black Saturday plume, J. Geophys. Res., 117, D04204, doi:10.1029/2011JD017016, 2012.

Donnell, E. A., Fish, D. J., Dicks, E. M., and Thorpe, A. J.: Mechanisms for pollutant transport between the boundary layer and the free troposphere, J. Geophys. Res., 106, 7847–7856, doi:10.1029/2000JD900730, 2001.

European Space Agency: Envisat, MIPAS An instrument for atmospheric chemistry and climate research, ESA Publications Division, ESTEC, P. O. Box 299, 2200 AG Noordwijk, The Netherlands, SP-1229, 2000.

Fischer, H., Birk, M., Blom, C., Carli, B., Carlotti, M., von Clarmann, T., Delbouille, L., Dudhia, A., Ehhalt, D., Endemann, M., Flaud, J. M., Gessner, R., Kleinert, A., Koopman, R., Langen, J., López-Puertas, M., Mosner, P., Nett, H., Oelhaf, H., Perron, G., Remedios, J.,

Ridolfi, M., Stiller, G., and Zander, R.: MIPAS: an instrument for atmospheric and climate research, Atmos. Chem. Phys., 8, 2151–2188, doi:10.5194/acp-8-2151-2008, 2008.

Funke, B., López-Puertas, M., García-Comas, M., Stiller, G. P., von Clarmann, T., Höpfner, M., Glatthor, N., Grabowski, U., Kellmann, S., and Linden, A.: Carbon monoxide distributions from the upper troposphere to the mesosphere inferred from 4.7 µm non-local thermal equilibrium emissions measured by MIPAS on Envisat, Atmos. Chem. Phys., 9, 2387–2411, doi:10.5194/acp-9-2387-2009, 2009.

Glatthor, N., von Clarmann, T., Stiller, G. P., Funke, B., Koukouli, M. E., Fischer, H., Grabowski, U., Höpfner, M., Kellmann, S., and Linden, A.: Large-scale upper tropospheric pollution observed by MIPAS HCN and C_2H_6 global distributions, Atmos. Chem. Phys., 9, 9619–9634, doi:10.5194/acp-9-9619-2009, 2009.

Grutter, M., Glatthor, N., Stiller, G. P., Fischer, H., Grabowski, U., Höpfner, M., Kellmann, S., Linden, A., and von Clarmann, T.: Global distribution and variability of formic acid as observed by MIPAS-ENVISAT, J. Geophys. Res., 115, D10303, doi:10.1029/2009JD012980, 2010.

Höpfner, M., von Clarmann, T., Fischer, H., Glatthor, N., Grabowski, U., Kellmann, S., Kiefer, M., Linden, A., Mengistu Tsidu, G., Milz, M., Steck, T., Stiller, G. P., Wang, D.-Y., and Funke, B.: First spaceborne observations of Antarctic stratospheric $ClONO_2$ recovery: Austral spring 2002, J. Geophys. Res., 109, D11308, doi:10.1029/2004JD004609, 2004.

Kahn, R. A., Li, W.-H., Moroney, C., Diner, D. J., Martonchik, J. V., and Fishbein, E.: Aerosol source plume physical characteristics from space-based multiangle imaging, J. Geophys. Res., 112, D11205, doi:10.1029/2006JD007647, 2007.

Kaminski, J. W., Neary, L., Struzewska, J., McConnell, J. C., Lupu, A., Jarosz, J., Toyota, K., Gong, S. L., Côté, J., Liu, X., Chance, K., and Richter, A.: GEM-AQ, an on-line global multiscale chemical weather modelling system: model description and evaluation of gas phase chemistry processes, Atmos. Chem. Phys., 8, 3255–3281, doi:10.5194/acp-8-3255-2008, 2008.

Keene, W. C. and Galloway, J. N.: The biogeochemical cycling of formic and acetic acids through the troposphere: an overview of current understanding, Tellus B, 40, 322–334, 1988.

Li, Q., Jacob, D. J., Yantosca, R. M., Heald, C. L., Singh, H. B., Koike, M., Zhao. Y., Sachse, G. W., and Streets, D. G.: A global three-dimensional model analysis of the atmospheric budgets of HCN and CH_3CN: constraints from aircraft and ground measurements, J. Geophys. Res., 108, 8827, doi:10.1029/2002JD003075, 2003.

Lupu, A., Kaminski, J. W., Neary, L., McConnell, J. C., Toyota, K., Rinsland, C. P., Bernath, P. F., Walker, K. A., Boone, C. D., Nagahama, Y., and Suzuki, K.: Hydrogen cyanide in the upper troposphere: GEM-AQ simulation and comparison with ACE-FTS observations, Atmos. Chem. Phys., 9, 4301–4313, doi:10.5194/acp-9-4301-2009, 2009.

Mu, M., Randerson, J. T., van der Werf, G. R., Giglio, L., Kasibhatla, P., Morton, D., Collatz, G. J., DeFries R. S., Hyer, E. J., Prins, E. M., Griffith, D. W. T., Wunch, D., Toon, G. C., Sherlock, V., and Wennberg, P. O.: Daily and 3-hourly variability in global fire emissions and consequences for atmospheric model predictions of carbon monoxide, J. Geophys. Res., 116, D24303, doi:10.1029/2011JD016245, 2011.

Nett, H., Perron, G., Sanchez, M., Burgess, A., and Mossner, P.: MIPAS inflight calibration and processor validation, in: ENVISAT Calibration Review – Proc. of the European Workshop, 9–13 September 2002, ESTEC, Noordwijk, The Netherlands, CD-ROM, vol. SP-520, edited by: Sawaya-Lacoste, H., ESA Publications Division, ESTEC, Postbus 299, 2200 AG Noordwijk, The Netherlands, 2002.

Park, M., Randel, W. J., Emmons, L. K., Bernath, P. F., Walker, K. A., and Boone, C. D.: Chemical isolation in the Asian monsoon anticyclone observed in Atmospheric Chemistry Experiment (ACE-FTS) data, Atmos. Chem. Phys., 8, 757–764, doi:10.5194/acp-8-757-2008, 2008.

Pumphrey, H. C., Santee, M. L., Livesey, N. J., Schwartz, M. J., and Read, W. G.: Microwave Limb Sounder observations of biomass-burning products from the Australian bush fires of February 2009, Atmos. Chem. Phys., 11, 6285–6296, doi:10.5194/acp-11-6285-2011, 2011.

Remedios, J. J., Leigh, R. J., Waterfall, A. M., Moore, D. P., Sembhi, H., Parkes, I., Greenhough, J., Chipperfield, M.P., and Hauglustaine, D.: MIPAS reference atmospheres and comparisons to V4.61/V4.62 MIPAS level 2 geophysical data sets, Atmos. Chem. Phys. Discuss., 7, 9973–10017, doi:10.5194/acpd-7-9973-2007, 2007.

Rinsland, C. P., Meier, A., Griffith D. W. T., and Chiou, L. S.: Ground-based measurements of tropospheric CO, C_2H_6, and HCN from Australia at 34° S latitude during 1997–1998, J. Geophys. Res., 106, 20913–20924, 2001.

Rinsland, C. P., Dufour, G., Boone, C. D., and Bernath, P. F.: Atmospheric Chemistry Experiment (ACE) measurements of elevated Southern Hemisphere upper tropospheric CO, C_2H_6, HCN, and C_2H_2 mixing ratios from biomass burning emissions and long range transport, Geophys. Res. Lett., 32, L20803, doi:10.1029/2005GL024214, 2005.

Rudolph, J., Ehhalt, D. H., and Khedim, A.: Vertical profiles of acetylene in the troposphere and stratosphere, J. Atmos. Chem., 2, 117–124, 1984.

Siddaway, J. M. and Petelina, S. V.: Transport and evolution of the 2009 Australian Black Saturday bushfire smoke in the lower stratosphere observed by OSIRIS on Odin, J. Geophys. Res., 116, D06203, doi:10.1029/2010JD015162, 2011.

Singh, H. B., Herlth, D., Kolyer, R., Chatfield, R., Viezee, W., Salas, L. J., Chen, Y., Bradshaw, J. D., Sandholm, S. T., Talbot, R., Gregory, G. L., Anderson, B., Sachse, G. W., Browell, E., Bachmeier, A. S., Blake, D. R., Heikes, B., Jacob, D., and H. E. Fuelberg: Impact of biomass burning emissions on the composition of the South Atlantic troposphere: reactive nitrogen and ozone, J. Geophys. Res., 101, 24203–24219, 1996.

Singh, H. B., Viezee, W., Chen, Y., Bradshaw, J., Sandholm, S., Blake, D., Blake, N., Heikes, B., Snow, J., Talbot, R., Browell, E., Gregory, G., Sachse, G., and Vay, S.: Biomass burning influences on the composition of the remote South Pacific troposphere: analysis based on observations from PEM-Tropics-A, Atmos. Environ., 34, 635–644, 2000.

Singh, H. B., Salas, L., Herlth, D., Kolyer, R., Czech, E., Viezee, W., Li, Q., Jacob, D. J., Blake, D., Sachse, G., Harward, C. N., Fuelberg, H., Kiley, C. M., Zhao, Y., and Kondo, Y.: In situ measurements of HCN and CH_3CN over the Pacific Ocean: sources, sinks and budgets, J. Geophys. Res., 108, 8795–8808, doi:10.1029/2002JD003006, 2003.

Stavrakou, T., Müller, J.-F., Peeters, J., Razavi, A., Clarisse, L., Clerbaux, C., Coheur, P.-F., Hurtmans, D., De Mazière, M., Vigouroux, C., Deutscher, N. M., Griffith, D. W. T. Jones, N., and Paton-Walsh, C.: Satellite evidence for a large source of formic acid from boreal and tropical forests, Nature Geosci., 5, 26–30, doi:10.1038/NGEO1354, 2012.

Steck, T.: Methods for determining regularization for atmospheric retrieval problems, Appl. Optics, 41, 1788–1797, 2002.

Stiller, G. P. (Ed.): The Karlsruhe Optimized and Precise Radiative transfer Algorithm (KOPRA), Institut für Meteorologie und Klimaforschung, Forschungszentrum Karlsruhe GmbH, 2000.

Teague, B., McLeod, D., and Pascoe, S.: 2009 Victorian Bushfires Royal Commission – Final Report, Tech. rep., http://www.royalcommission.vic.gov.au/Commission-Reports/Final-Report, 2010.

Tolhurst, K.: Report on the Physical Nature of the Victorian Fires occurring on 7th February 2009, Commissioned report to the Victorian Bushfires Royal Commission, 18 pp., http://www.royalcommission.vic.gov.au/getdoc/5905c7bb-48f1-4d1d-a819bb2477c084c1/EXP.003.001.0017.pdf, 2009.

Tolhurst, K. G., Shields, B. J., and Chong, D. M.: PHOENIX: development and application of a bushfire risk management tool, Australian Journal of Emergency Management, 23, 47–54, 2008.

Trentmann, J., Luderer, G., Winterrath, T., Fromm, M. D., Servranckx, R., Textor, C., Herzog, M., Graf, H.-F., and Andreae, M. O.: Modeling of biomass smoke injection into the lower stratosphere by a large forest fire (Part I): reference simulation, Atmos. Chem. Phys., 6, 5247–5260, doi:10.5194/acp-6-5247-2006, 2006.

van der Werf, G. R., Randerson, J. T., Giglio, L., Collatz, G. J., Mu, M., Kasibhatla, P. S., Morton, D. C., DeFries, R. S., Jin, Y., and van Leeuwen, T. T.: Global fire emissions and the contribution of deforestation, savanna, forest, agricultural, and peat fires (1997–2009), Atmos. Chem. Phys., 10, 11707–11735, doi:10.5194/acp-10-11707-2010, 2010.

von Clarmann, T., Glatthor, N., Grabowski, U., Höpfner, M., Kellmann, S., Kiefer, M., Linden, A., Mengistu Tsidu, G., Milz, M., Steck, T., Stiller, G. P., Wang, D.-Y., Fischer, H., Funke, B., Gil-López, S., and López-Puertas, M.: Retrieval of temperature and tangent altitude pointing from limb emission spectra recorded from space by the michelson interferometer for passive atmospheric sounding (MIPAS), J. Geophys. Res., 108, 4736–4750, doi:10.1029/2003JD003602, 2003.

von Clarmann, T., Glatthor, N., Koukouli, M. E., Stiller, G. P., Funke, B., Grabowski, U., Höpfner, M., Kellmann, S., Linden, A., Milz, M., Steck, T., and Fischer, H.: MIPAS measurements of upper tropospheric C_2H_6 and O_3 during the southern hemispheric biomass burning season in 2003, Atmos. Chem. Phys., 7, 5861–5872, doi:10.5194/acp-7-5861-2007, 2007.

von Clarmann, T., Höpfner, M., Kellmann, S., Linden, A., Chauhan, S., Funke, B., Grabowski, U., Glatthor, N., Kiefer, M., Schieferdecker, T., Stiller, G. P., and Versick, S.: Retrieval of temperature, H_2O, O_3, HNO_3, CH_4, N_2O, $ClONO_2$ and ClO from MIPAS reduced resolution nominal mode limb emission measurements, Atmos. Meas. Tech., 2, 159–175, doi:10.5194/amt-2-159-2009, 2009.

Wiegele, A., Glatthor, N., Höpfner, M., Grabowski, U., Kellmann, S., Linden, A., Stiller, G., and von Clarmann, T.: Global distributions of C_2H_6, C_2H_2, HCN, and PAN retrieved from MIPAS reduced spectral resolution measurements, Atmos. Meas. Tech., 5, 723–734, doi:10.5194/amt-5-723-2012, 2012.

Xiao, Y., Jacob, D. J., and Turquety, S.: Atmospheric acetylene and its relationship with CO as an indicator of air mass age, J. Geophys. Res., 112, D12305, doi:10.1029/2006JD008268, 2007.

Yokelson, R. J., Urbanski, S. P., Atlas, E. L., Toohey, D. W., Alvarado, E. C., Crounse, J. D., Wennberg, P. O., Fisher, M. E., Wold, C. E., Campos, T. L., Adachi, K., Buseck, P. R., and Hao, W. M.: Emissions from forest fires near Mexico City, Atmos. Chem. Phys., 7, 5569–5584, doi:10.5194/acp-7-5569-2007, 2007.

Table 1. Mean values, scatter and upper thresholds for outliers of southern hemispheric C_2H_2, HCN, and HCOOH measured by MIPAS during background conditions, averaged over the period 1 January to 7 February 2009.

Gas	height [km]	mean vmr [pptv]	std dev [pptv]	mean + 3σ
C_2H_2	15	3.0	17.8	56.4
”	18	−8.1	9.4	20.1
”	21	−3.2	6.8	17.2
HCN	15	243.3	40.9	365.7
”	18	254.8	36.7	364.9
”	21	229.1	34.9	333.8
HCOOH	15	14.5	18.8	70.9
”	18	8.2	19.8	67.6
”	21	8.4	17.8	61.8

Table 2. Maximum MIPAS and GEM-AQ C_2H_2 amounts of selected days in the area 53–20° S, 120° E–20° W.

Day	height [km]	MIPAS max-vmr [pptv]	GEM-AQ max-vmr [pptv]
8 Feb 2009	12	**111.7**	466.0
	15	43.1	**1109.8**
	18	17.3	885.2
	21	16.4	124.5
9 Feb 2009	12	58.0	311.7
	15	**152.7**	**846.4**
	18	142.6	690.7
	21	26.8	183.3
10 Feb 2009	12	**325.5**	230.3
	15	109.5	**832.2**
	18	69.9	828.8
	21	23.9	230.1
11 Feb 2009	12	106.5	249.3
	15	**222.5**	684.4
	18	183.0	**819.6**
	21	45.3	252.1
14 Feb 2009	12	120.9	121.4
	15	214.8	**370.4**
	18	**279.7**	284.6
	21	66.9	123.9
17 Feb 2009	12	79.1	65.0
	15	**222.7**	**203.4**
	18	201.8	177.8
	21	60.3	75.6
20 Feb 2009	12	105.9	40.6
	15	**131.5**	**69.5**
	18	89.6	55.4
	21	35.3	33.3

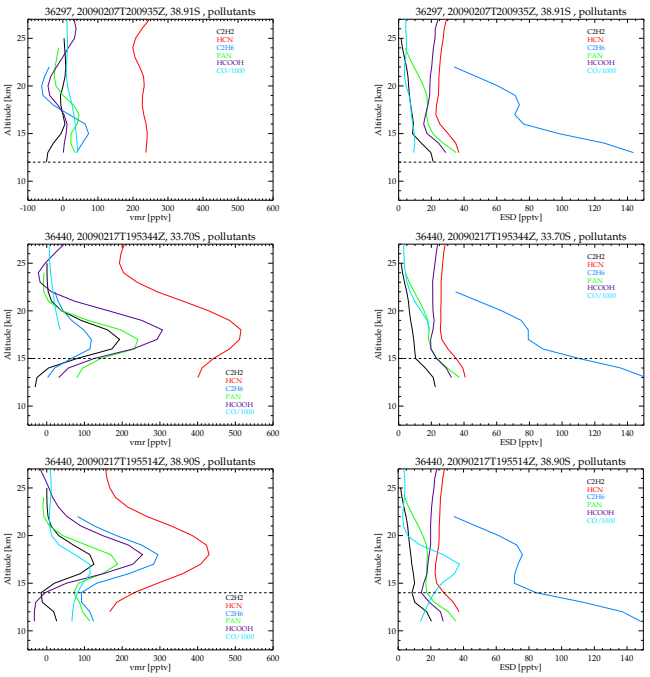

Fig. 1. Upper row: (left) VMR-profiles of C_2H_2, HCN, C_2H_6, PAN, HCOOH and CO (colour coded, see legend), measured by MIPAS on 7 February 2009, in an unpolluted atmosphere over the Central South Pacific. CO amounts are in ppbv and scaled down by a factor of 1000. (right) Corresponding estimated standard deviations. Dashed line indicates the altitude of the thermal tropopause. Middle and lower row: same as upper row, but for MIPAS mesurements on 17 February 2009, inside the plume of the Australian bush fires. The measurements were made at 38.9° S, 151.7° W (top), 33.7° S, 146.8° W (middle) and at 38.9° S, 148.1° W (bottom).

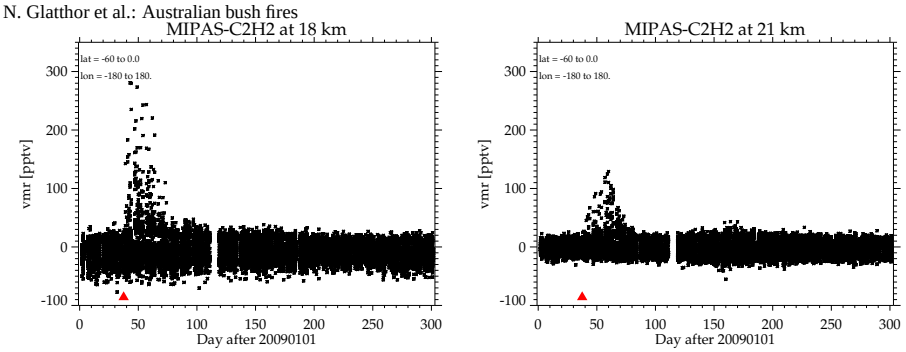

Fig. 2. MIPAS C_2H_2 data in the latitude band 60° S to 0° N for the time period 1 January to 31 October 2009, measured at 18 km (left) and 21 km altitude (right). The red triangle indicates the date of the outbreak of the Australian bush fires (7 February).

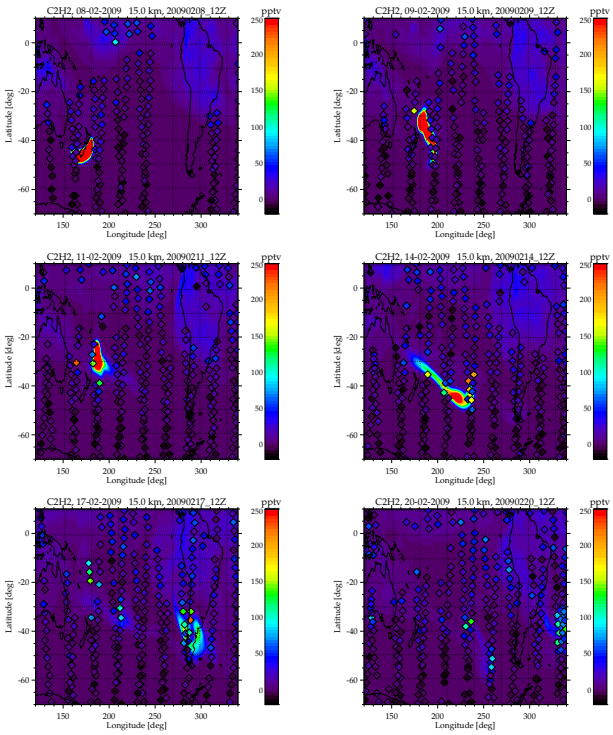

Fig. 3. MIPAS C_2H_2 data at 15 km altitude (diamonds), measured on 8, 9, 11, 14, 17 and 20 February 2009 (top left to bottom right). Background areas are GEM-AQ C_2H_2 model distributions for 12:00 UT of the respective days. Red diamonds with black pluses inside indicate MIPAS vmrs higher than 250 pptv, and red areas are GEM-AQ data equal or higher than 250 pptv.

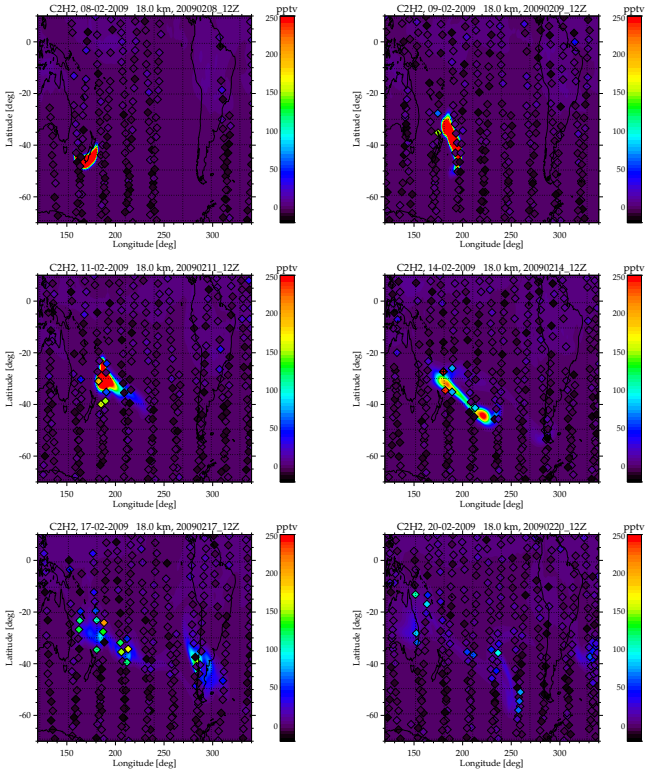

Fig. 4. Measured and modelled C_2H_2 at 18 km altitude. For more details see Fig. 3.

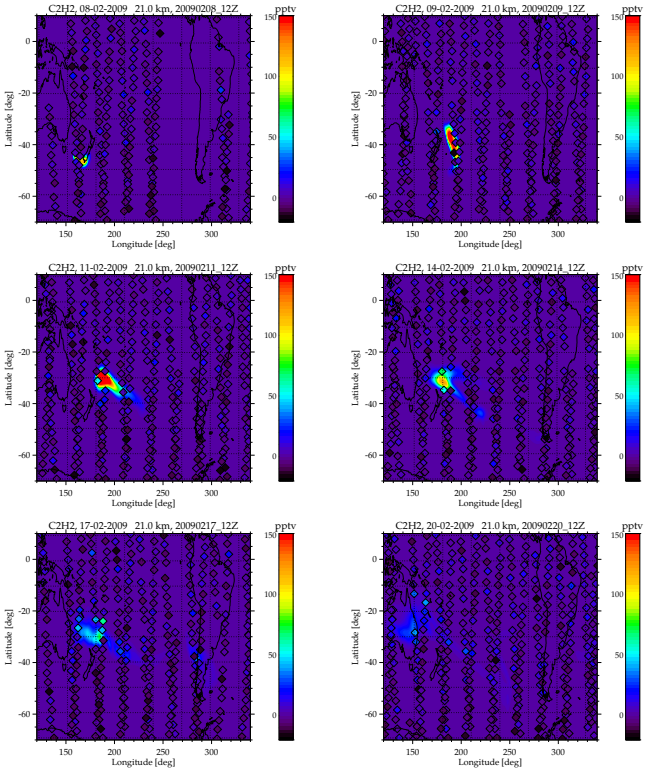

Fig. 5. Measured and modelled C_2H_2 at 21 km altitude. Red areas are GEM-AQ data equal or higher than 150 pptv. For more details see Fig. 3.

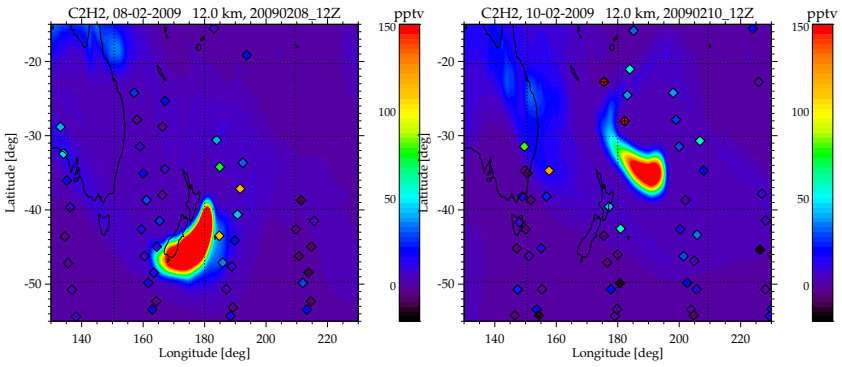

Fig. 6. MIPAS C_2H_2 data at 12 km altitude (diamonds), measured on 8 February (left) and 10 February (right) 2009. Background areas are GEM-AQ C_2H_2 model distributions for 12:00 UT. Red diamonds with black pluses inside indicate MIPAS vmrs higher than 150 pptv, and red areas are GEM-AQ data equal or higher than 150 pptv.

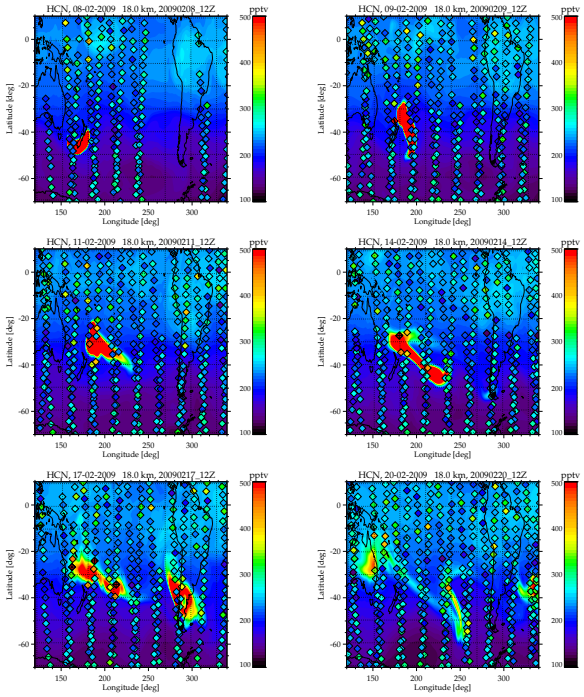

Fig. 7. MIPAS HCN data at 18 km altitude (diamonds), measured on 8, 9, 11, 14, 17 and 20 February 2009 (top left to bottom right). Background areas are GEM-AQ HCN model distributions for 12:00 UT of the respective days. Red diamonds with black pluses inside indicate MIPAS vmrs higher than 500 pptv, and red areas are GEM-AQ data equal or higher than 500 pptv.

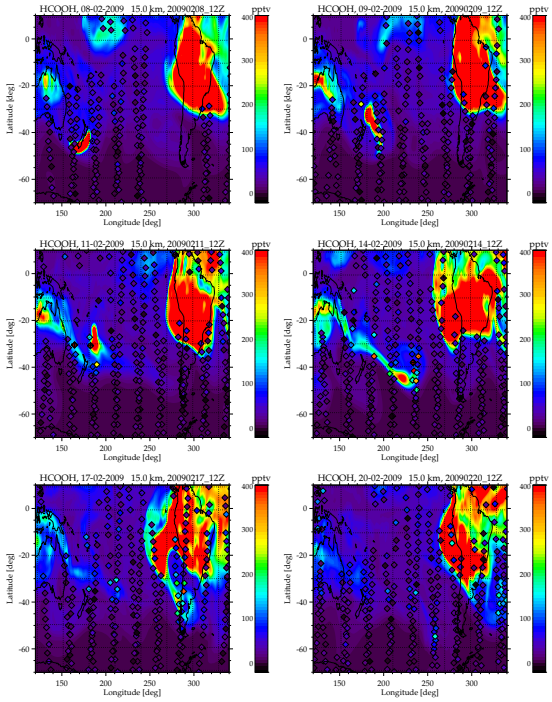

Fig. 8. MIPAS HCOOH data at 15 km altitude (diamonds), measured on 8, 9, 11, 14, 17 and 20 February 2009 (top left to bottom right). Background areas are GEM-AQ HCOOH model distributions for 12:00 UT of the respective days scaled down by a factor of 0.3. Red diamonds with black pluses inside indicate MIPAS vmrs higher than 400 pptv, and red areas are GEM-AQ data equal or higher than 1333 pptv.

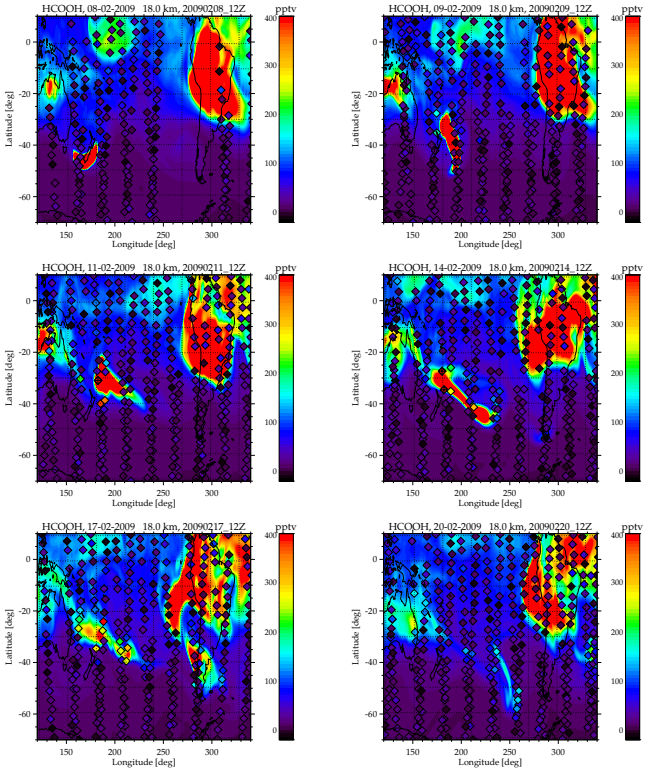

Fig. 9. Measured and modelled HCOOH at 18 km altitude. Red diamonds with black pluses inside indicate MIPAS vmrs higher than 400 pptv, and red areas are GEM-AQ data (unscaled) equal or higher than 400 pptv. For more details see Fig. 8.

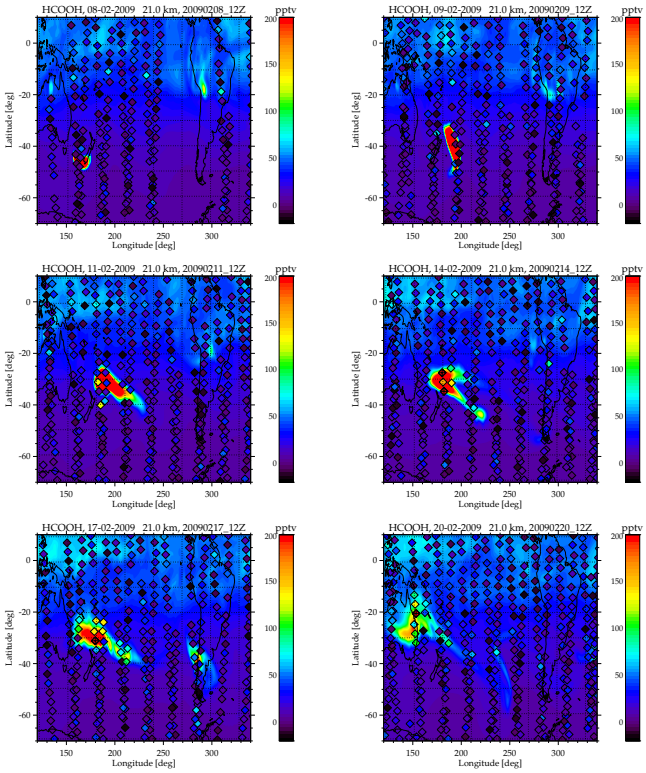

Fig. 10. Measured and modelled HCOOH at 21 km altitude. Red diamonds with black pluses inside indicate MIPAS vmrs higher than 200 pptv, and red areas are GEM-AQ data (unscaled) equal or higher than 200 pptv. For more details see Fig. 8.

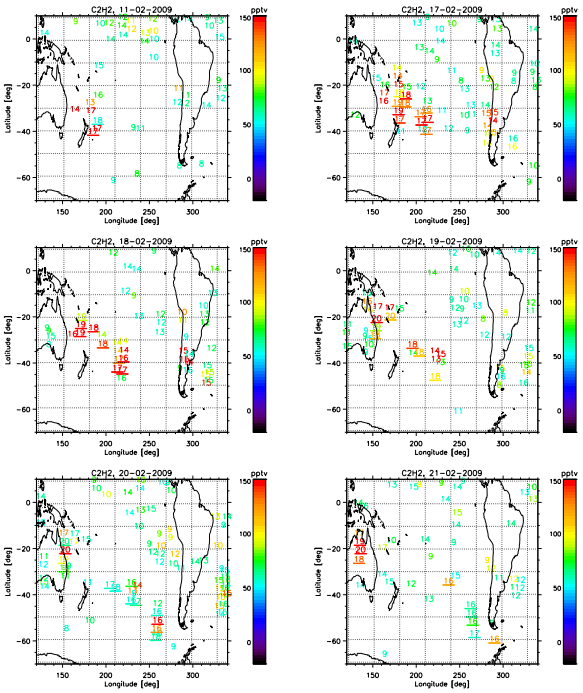

Fig. 11. Geometrical height (in km, denoted by numbers) of maxima (in vmr, colour coded) of measured C_2H_2 profiles from 11, 17, 18, 19, 20 and 21 February 2009 (top left to bottom right). Only maxima above 50 pptv are presented. Maxima, which are 1 km or more above the tropopause, derived from MIPAS temperature profiles, are underlined.

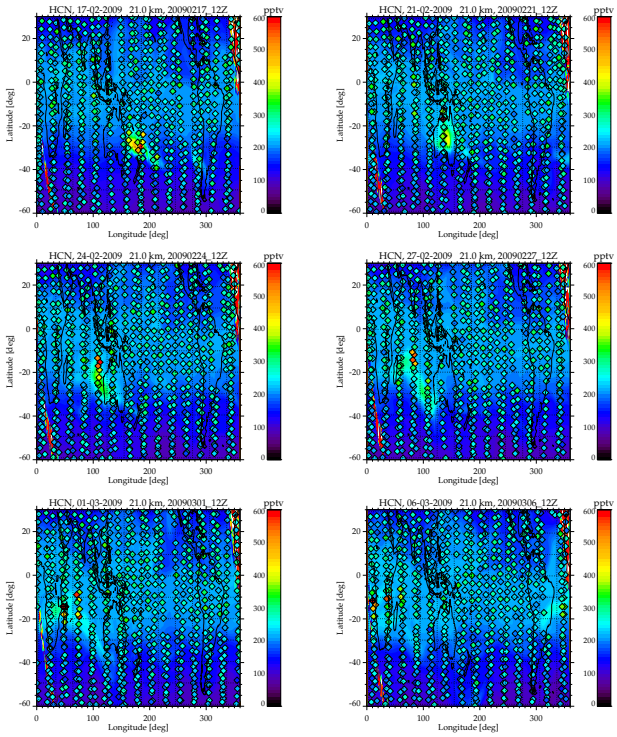

Fig. 12. MIPAS HCN data (diamonds) at 21 km altitude, measured on 17, 21, 24, 27 February and on 1 and 6 March 2009. Background areas are GEM-AQ HCN model distributions for 12:00 UT of the respective days. Red diamonds with black pluses inside indicate MIPAS vmrs higher than 600 pptv.